Investigation of hydrogen bonding in neat dimethyl sulfoxide and binary mixture (dimethyl sulfoxide + water) by concentration-dependent Raman study and *ab initio* calculation*

Ouyang Shun-Li(欧阳顺利)[a], Wu Nan-Nan(吴楠楠)[b], Liu Jing-Yao(刘靖尧)[b], Sun Cheng-Lin(孙成林)[a]†, Li Zuo-Wei(里佐威)[a]‡, and Gao Shu-Qin(高淑琴)[a]

[a] *College of Physics, Jilin University, Changchun* 130012, *China*
[b] *Institute of Theoretical Chemistry, State Key Laboratory of Theoretical and Computational Chemistry, Jilin University, Changchun* 130023, *China*

(Received 22 May 2010; revised manuscript received 3 July 2010)

In this study, our vibrational spectroscopic analysis is made on hydrogen-bonding between dimethyl sulfoxide and water comprises both experimental Raman spectra and *ab initio* calculations on structures of various dimethyl sulfoxide/water clusters with increasing water content. The Raman peak position of the v(S=O) stretching mode of dimethyl sulfoxide serves as a probe for monitoring the degree of hydrogen-bonding between dimethyl sulfoxide and water. In addition, the two vibrational modes, namely, the CH_3 symmetric stretching mode and the CH_3 asymmetric stretching mode have been analysed under different concentrations. We relate the computational results to the experimental vibrational wavenumber trends that are observed in our concentration-dependent Raman study. The combination of experimental Raman data with *ab initio* calculation leads to a better knowledge of the nature of the hydrogen bonding and the structures of the hydrogen-bonded complexes studied.

Keywords: hydrogen-bonding, Raman spectroscopy, *ab initio* calculations, dimethl sulphoxide

PACC: 3120, 3220F

1. Introduction

The phenomenon of hydrogen bonding is vital in nature.[1] Hydrogen bonds play key roles on some functionalities for many biological systems, soft materials of molecular systems, and chemical reactions in hydrogen-bonding solutions. Recently, organic crystal engineering has emerged as one of the important areas of research, where hydrogen bonding plays a very important role.[2] An important strategy has been to take advantage of hydrogen bond interaction between molecules[3−5] and to generate a variety of super molecular assemblies.[6,7] Although hydrogen bonds are weak, they give considerable stability to the protein molecule and also stabilize the structure of ribonucleic acid (RNA) and deoxyribonucleic acid (DNA) by forming hydrogen bonds between the pyrimidine and purine bases. A hydrogen bond is formed between an electron-rich element or more electronegative element (such as N, O, or Cl) and the H atom of a hydrogen donor solvent.[8−11] So various experimental methods are employed to characterize hydrogen bonds.[12] For the solid state materials, nuclear magnetic resonance (NMR) spectroscopy is one of the preferred methods.[13] In the gas phase, vibrational spectroscopy on molecular beams is often performed, which allows one to assess information of isolated hydrogen-bonded complexes.[14] For the liquid state substances, where the formation and cleavage of such as IR and Raman spectra are ideally suitable to detect hydrogen-bonding because they cover both structural and dynamic aspects.[15−19] However, as compared to IR absorption spectroscopy, Raman spectroscopy can be used easily for aqueous samples because the strong infrared absorption of water may mask other signals. Therefore, it is suitable for our samples (dimethyl sulfoxide/water).

Dimethyl sulfoxide (DMSO) is a wonderful,

*Project supported by the National Natural Science Foundation of China (Grant Nos. 10774057 and 10974067) and the Graduate Innovation Fund of Jilin University.

†Corresponding author. E-mail: chenglin@jlu.edu.cn
‡Corresponding author. E-mail: zuoweili@163.com

© 2010 Chinese Physical Society and IOP Publishing Ltd

rapidly acting solvent.[20] It dissolves many compounds that are insoluble in most other liquids and it causes increases in the rates of bimolecular reactions over the rates in protic solvents. DMSO is also an important reactant and pharmaceutical agent.[21] The important chemical properties of DMSO are related to the hydrogen bonds forming between DMSO and other compounds, within which the hydrogen bond forming with water has attracted particular attention of researchers. Therefore, there are numerous experimental and theoretical studies of water/DMSO mixture available.[22−30] In these studies, the experimental techniques are used, such as infrared absorption,[24,25] Raman scattering[24] or NMR as well as x-ray scattering.[23,26−29] However, a reasonably good correlation between the observed spectra and optimized geometry is still lacking. Wulf and Ludwing[22] have used a combination of Fourier transform infrared (FTIR), NMR spectroscopy and *ab initio* calculations to study the structure and dynamics of water (H_2O) in DMSO, but they focused on confined water molecules in DMSO.[23]

In this study, Raman spectra of liquid DMSO and its binary mixtures are recorded and analysed to obtain information of hydrogen bond formation. *Ab initio* calculations for optimized geometries are also made in order to understand and explain the spectral features observed in the binary mixture with varying mole fraction of the reference system, DMSO.

2. Methods

2.1. Samples and procedures

The sample of DMSO was obtained from Aldrich Co. and without further purification afterwards. For preparing the binary mixture, triple-distilled water was used as solvent. The binary mixtures of DMSO in H_2O were prepared with various mole fractions of the solute.

2.2. Instruments and measurement

The micro Raman spectrometer (Renishaw InVia Raman microscope) equipped with a 514.5-nm Ar^+ ion excitation laser (Spectra Physics 163-M42) was used to obtain Raman spectra. The 5× objective (LEICA DMLM 0.12NA) was used for both laser illumination and Raman backscattering detection. The excitation power of 5.6 mW and exposure time (CCD integration times) of 10 s were used to collect all Raman spectra.

Raman spectra are recorded in the region, 1000∼1100 cm^{-1} for the neat as well as for seven different mole fractions, C = 0.1, 0.2, 0.3, 0.4, 0.5, 0.6 and 0.7 of the reference system, DMSO in the binary mixture (DMSO+H_2O). These spectra are presented in Fig. 1. Raman spectra are recorded in the region, 2900∼3100 cm^{-1} also for the neat as well as for the binary mixture with same mole fractions. These spectra are presented in Fig. 2. A detailed line shape analysis in each case and several hitherto unexplored aspects will be presented later.

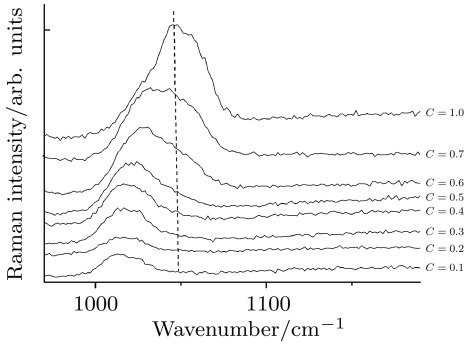


Fig. 1. The Raman spectra in the region, 1000–1100 cm^{-1} for neat DMSO and its binary mixture, DMSO+H_2O at seven different mole fractions of DMSO, C = 1.0, 0.7, 0.6, 0.5, 0.4, 0.3, 0.2, 0.1.

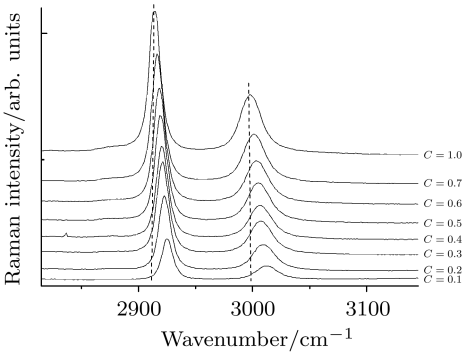


Fig. 2. The Raman spectra in the region, 2900–3100 cm^{-1} for neat DMSO and its binary mixture, DMSO+H_2O at seven different mole fractions of DMSO, C = 1.0, 0.7, 0.6, 0.5, 0.4, 0.3, 0.2, 0.1.

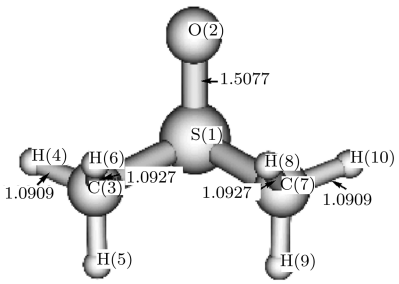
2.3. Computational methods

The ground state geometries for DMSO and its various hydrogen bonded complexes are optimized at the second order MΦler-pleset perturbation MP2 method employing the 6-311+G(d,p) basis set. Vibrational frequency calculations are performed to verify whether they are minima with all positive frequencies. All calculations using the Gaussian 03 program.[31]

3. Results and discussion

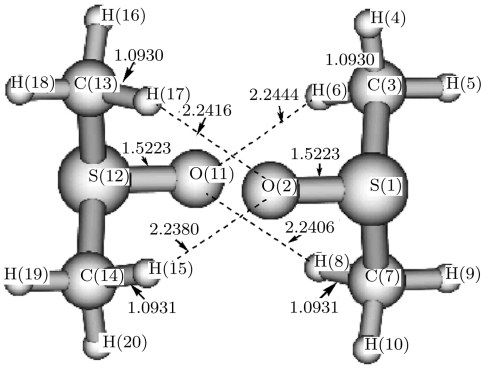
3.1. Optimized geometries of the neat and binary mixtures

The basic aim of *ab initio* calculations of optimized geometries for the reference molecule, DMSO, and its several complexes are to understand the observed spectral features of neat DMSO, its self-associated dimer, and its several complexes with the H_2O. All of the electronic structure calculations are carried out by the Gaussian 03 program, the ground state geometries for neat DMSO, its self-associated dimer, and several complexes with H_2O are optimized by using the MP2 method (second order MΦller-pleset perturbation theory) with the 6-311+G(d,p) basis set. The optimized geometries obtained from the *ab initio* calculations for DMSO and all other structures are presented in Fig. 3. The total energies for the monomers (DMSO and H_2O) and self-associated dimer of DMSO as well as the hydrogen-bonded complexes of DMSO quoted in Hartree in the optimized structures are depicted in Fig. 3. The total energies of the H_2O monomer is calculated to be –76.27472 Hartree (not shown in Fig. 3). The total energies of the self-association and the hydrogen-bonded complexes are less than the sum of energies of the individual monomers, which clearly indicates that stable dimers and complexes are formed. The dimer is shown in Fig. 3(b). The hydrogen-bonded complexes of DMSO with one water molecule are calculated in two different configurations as shown in Figs. 3(c) and 3(d), respectively. The ($DMSOW_1$-A) complex depicted in Fig. 3(c) exhibits a shorter O $\cdots$ H–O bond length (1.8076 Å) as compared with the ($DMSOW_1$-B) complex (1.8285 Å), which indicates the formation of a stronger hydrogen bond. The angle of O10-H12-O11 in complex $DMSOW_1$-A is 155.0° and the angle of O10-H13-O11 in complex $DMSOW_1$-B is 176.9°. The hydrogen-bonded complex of DMSO with two molecules is calculated in the configuration as shown in Fig. 3(e). In this case, the H atom of the OH group of two water molecules forms hydrogen bonds with the same O atom of the reference molecule DMSO, the hydrogen bond lengths are 1.8260 Å and 1.8273 Å, respectively.

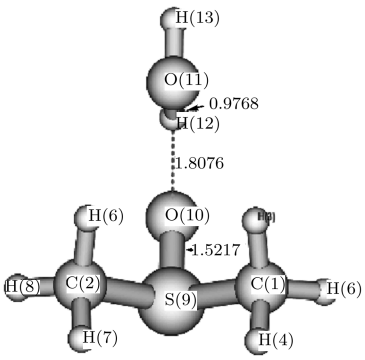


DMSO

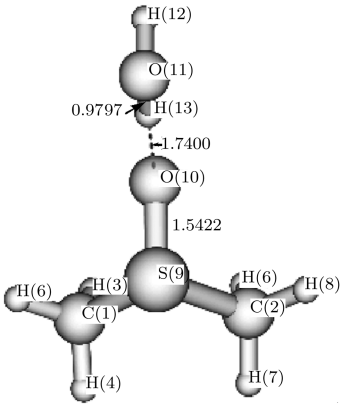
(a) $E = -552.2623599$ Hartree



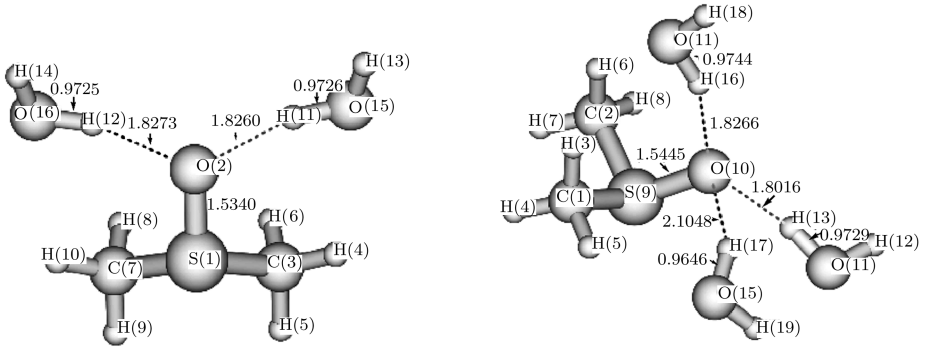
(b) $E = -1104.5471202$ Hartree



(c) $E = -628.5550168$ Hartree



(d) $E = -628.5512952$ Hartree



(e) $E = -704.8429788$ Hartree (f) $E = -781.1335226$ Hartree

Fig. 3. Optimized geometries obtained from *ab initio* calculations for: (a) DMSO, (b) self-associated dimer of DMSO, (c) hydrogen-bonded complex of DMSO forming one hydrogen bond with one water molecule-A-configuration, (d) hydrogen-bonded complex of DMSO forming one hydrogen bond with one water molecule-B-configuration, (e) hydrogen-bonded complex of DMSO forming two hydrogen bonds with two water molecules, (f) hydrogen-bonded complex of DMSO forming three hydrogen bonds with three water molecules. Selected distances (Å, 1 Å = 0.1 nm) are indicated.

The angles of O2–H12–O16 and O2–H11–O16 are 161.6° and 161.8°, respectively. Similar to the ($DMSOW_2$) complex, hydrogen-bonding of three water molecules to DMSO can result in the formation of the $DMSOW_3$ clusters as depicted in Fig. 3(f). The hydrogen bond lengths in the ($DMSOW_3$) complex are 1.8016, 1.8266, and 2.1048 Å, respectively. The angles of O10–H16–O14, O10–H19–O11 and O10–H17–O15 are 155.0, 164.0°, and 145.8°, respectively. As a result, the bond length of S=O bond in the monomer, the ($DMSOW_1$-A) complex, the ($DMSOW_1$-B) complex, the ($DMSOW_2$) complex and the ($DMSOW_3$) complex are 1.50077, 1.5217, 1.5173, 1.5340 and 1.5445 Å, respectively. This has a very intriguing influence on the spectral features in solution, which will be discussed in detail in the relevant sections.

3.2. Concentration dependence of wavenumber shifts for v (S=O) stretching mode

The variation of peak positions with concentration for one major Raman mode, namely v (S=O) stretching mode,[32] appears in the region 1000∼1100 cm^{-1} (as shown in Fig. 1). In this study, the Raman peak position of v (S=O) stretching mode serves as a probe for monitoring the degree of hydrogen-bonding between DMSO and water. The degree of hydrogen-bonding in this binary system varies with mixture composition. In water as solvent, there is a possibility for intermolecular hydrogen bond between the S=O stretching band of the DMSO and the hydroxyl proton of the water molecule. In neat DMSO, a dimer of DMSO is formed. With the addition of water, the hydrogen bond of the dimer is broken due to the formation of stronger hydrogen bond between water and DMSO. The theoretically calculated value of hydrogen bond for the DMSO dimer is 2.2416 Å, less than that between water and DMSO, which confirms the tendency of the hydrogen bond formation between DMSO and water. When water is added into the solute, it will form OH $\cdots$ O=S type hydrogen bond. When more water is added, more molecules of solute will be hydrogen-bonded. As a consequence, the peak position of the S=O stretching wavenumber is shifted to lower wavenumber for decreasing the concentration of DMSO (as shown in Table 1).

Table 1. Peak positions and linewidths (FWHM) of the peak corresponding to v (S=O) of neat DMSO and its hydrogen bonded complexes.

mole fraction(C) of acetone	peak position/cm^{-1}	linewidth (FWHM)
1.0	1046.5	46.2
0.7	1040.2	51.3
0.6	1039.6	49.6
0.5	1024.2	48.3
0.4	1019.5	44.6
0.3	1017.8	39.5
0.2	1016.3	35.8
0.1	1013.1	35

Hence, it can be concluded that the S=O band, after hydrogen bond formation with water, withdraws some charge density from the band and thereby in-

creases the force constant of the S=O stretch which, in turn, decreases v (S=O) stretching frequency.

3.3. Variation of peak positions in the region, 2900–3100 cm^{-1}

The Raman spectra in the region, 2900–3100 cm^{-1} presented in Fig. 2 shows two clear Raman bands. The first band at ∼2900 cm^{-1} has been assigned to the CH_3 symmetric stretching mode and the other one at ∼3000 cm^{-1} to the CH_3 asymmetric stretching mode.[32] The spectra for neat DMSO as well as seven mixtures with water at different concentrations are presented in Fig. 2 and peak positions for different concentrations are shown in Table 2.

Table 2. Peak positions corresponding to ∼2900 cm^{-1} and ∼3000 cm^{-1} (in neat DMSO) with varying concentration of the reference system, H_2O, as obtained from the measured Raman line profile.

mole fration (DMSO)	peak position/cm^{-1})	
	CH_3 symmetric stretching	CH_3 asymmetric stretching
1.0	2913.7	2997.5
0.7	2916.2	2999.9
0.6	2918.7	3002.5
0.5	2919.9	3004.9
0.4	2921.2	3006.2
0.3	2921.3	3007.4
0.2	2922.5	3009.9
0.1	2925.0	3012.4

3.3.1. The CH_3 symmetric stretching mode

The CH_3 symmetric stretching mode appears at ∼2900 cm^{-1}. The peak is quite sharp and it is expected to show systematic and detectable spectral variation because of environmental changes. In neat DMSO, a dimer of it is formed. In this case, the H atom of the OH group of DMSO forms hydrogen bonds with the O atom of the other DMSO [Fig. 3(b)]. As the hydrogen bond of the dimer is broken with the addition of water, and no strong intermolecular hydrogen bonding occurs between the solute and the solvent through this mode, the peak position is upshifted in water for decreasing concentration of DMSO.

3.3.2. The CH_3 asymmetric stretching mode

In the Raman spectra of neat DMSO, the CH_3 asymmetric stretching mode is observed at ∼3000 cm^{-1}. The shift in peak position of this mode is analysed for all the concentrations mentioned above. The peak position is upshifted in H_2O. The explanation for this trend is the same as in the case of the CH_3 symmetric stretching mode.

3.4. Variation of linewidth of v (S=O) stretching mode in DMSO with concentration

The variation of linewidth of the v(S=O) stretching mode in DMSO with concentration shows a decrease upon dilution, and the results are presented in Fig. 4.

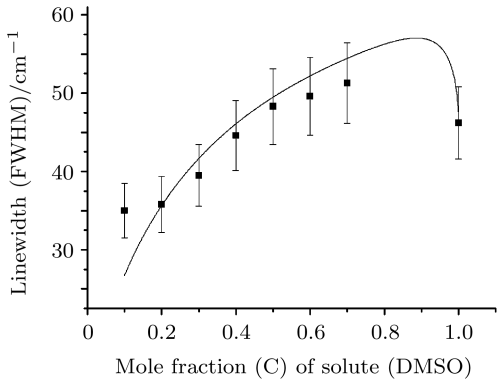


Fig. 4. The experimental data points for the Raman linewidth varying with concentration of the solute (DMSO) at mole fraction C for the v (S=O) stretching mode in the binary mixture and the solid line represents the fit obtained using Eq. (2).

The S=O bond of DMSO involves hydrogen bonding with the solvent molecule between the H atom of the water and the O atom of DMSO. The motion of the reference molecule, DMSO, is constrained owing to this hydrogen-bond formation with the solvent molecule. This would give rise to the phenomenon of motional narrowing as discussed by Oxtoby,[33] according to which the dipolar interaction and resonant energy transfer are mainly responsible for motional narrowing. An empirical model has been recently proposed by Ojha *et al.*[34] According to the model, the changes in the linewidth is not only due to the concentration fluctuation as in the model given by Bondarev and Mardaeva,[35] but also due to the change of the microviscosity at different relative concentrations of the solute and the solvent as well as the effect of concentration fluctuation as the microlevel. The viscosities of the different mixtures can be calculated using the relation:

$$\eta_{\text{mix}} = \eta_{\text{solute}} C + \eta_{\text{solvent}} (1 - C), \qquad (1)$$

where C is the mole fraction of the solute, and $\eta_{\rm solute}$ and $\eta_{\rm solvent}$ are the bulk viscosities of the solute and the solvent, respectively. The effect of viscosities can be visualized by comparing the viscosities of the solute and the solvent. The viscosities of DMSO and water are 1.996 cP and 1.002 cP, respectively. The variation of the linewidth with the concentration is given by the relation

$$\Gamma(C) = \Gamma_{\rm C} + \Gamma_{\rm i}(\eta_{\rm C}), \tag{2}$$

where $\Gamma_{\rm C}$ is the contribution due to the concentration fluctuation and $\Gamma_{\rm i}$ is the intrinsic linewidth given by

$$\Gamma_{\rm i}(\eta_{\rm C}) = \Gamma_{\rm i} \exp\left[-a\left(1 - \frac{\mu_2 \eta_{\rm C}}{\mu_1 \eta_{\rm solute}}\right)\right], \tag{3}$$

$$\Gamma_{\rm C} = 2\sqrt{2\ln 2}\Delta\Omega\sqrt{\frac{C(1-C)}{n}}, \tag{4}$$

$$\eta_{\rm m} = \eta\left[0.16 + 0.4\left(\frac{r_1}{r_2}\right)\right], \tag{5}$$

where μ_1 and μ_2 are microfriction parameters for neat liquid and the mixture, respectively; $\Delta\Omega$ is the amplitude of the wavenumber shift between the neat liquid and infinite dilution, n is the number of the neighbouring molecules influencing the reference mode. In the case of hydrogen-bonded system, the value of the Van der Waals radius of the terminal atom, through which the hydrogen bonding takes places, was taken as the solute radius r_1, and similarly the value of the Van der Waals radius of the terminal atom of the solvent involved in the hydrogen bonding was taken as the solvent radius r_2 for calculating microviscosity $\eta_{\rm mix}$ using Eq. (5). The parameter 'a' in Eq. (3) is an adjustable parameter which is basically vibrational-mode-dependent, and depends upon the polarizability of the vibrational mode under investigation. Therefore, it contributes to the linewidth. If $a = 1$ is substituted in Eq. (3), it still fits the qualitative trend, but by adjusting this parameter one can obtain a quantitative agreement with the experimental data. Furthermore, if $\eta_{\rm solute} > \eta_{\rm solvent}$, equation (2) would lead to line narrowing and for $\eta_{\rm solute} < \eta_{\rm solvent}$, it would lead to line broadening with decreasing mole fraction, C. It is also obvious from Eq. (2) that in the case of $\eta_{\rm solute} = \eta_{\rm solvent}$, $\Gamma_{\rm i}(\eta_{\rm C})$ becomes independent of the change in concentration.[34] In this study, $\eta_{\rm solute} > \eta_{\rm solvent}$, it gives rise to line narrowing with decreasing mole fraction. Therefore, in the present study, viscosity is the mainly factor that has influence on the linewidth of DMSO.

4. Conclusions

In this study, Raman spectra of DMSO have been taken for neat DMSO as well as binary mixture of it with water for different concentrations given. The peak position and Raman linewidth of the vibrational modes of DMSO have been analysed for all the different concentrations. From this study, it has been concluded that the structure of DMSO molecules is strongly connected with the hydrogen bonding in the solvent water, and the peak positions of the v(S=O) stretching mode wavenumber, the CH_3 symmetric stretching mode wavenumber and the CH_3 asymmetric stretching mode wavenumber are downshifted (upshifted) with the degree of hydrogen-bonding between DMSO and water. In addition, viscosity is the main factor that has influence on the linewidth of DMSO. The optimized geometries obtained by the *ab initio* calculations are good for explaining and supporting the changes in the spectral feature upon changing concentration of the solute in the binary mixture.

References

[1] Ojha A K, Srivastasva S K, Koster J, Shukla M K, Leszczyhski J, Asthana B P and Kiefer W 2004 *J. Mol. Struct.* **689** 127

[2] Vaidyanathan R, Natrajan S and Rao C N R 2002 *J. Mol. Struct.* **608** 123

[3] Jeffrey G A 1997 *An Introduction to Hydrogen Bonding* (New York: Oxford University Press)

[4] MacDonald J C and Whileride G M 1994 *Chem. Rev.* **94** 283

[5] Desiraju G R 1989 *Crystal Engineering: the Design of Organic Solid* (New York: Elsevier) p. 54

[6] Peddireddi V R, Ranganathan A and Ganesh K N 2001 *Org. Lett.* **3** 99

[7] Hobze P and Sponer J 1999 *Chem. Rev.* **30** 290

[8] Asthana B P, Takahashi H and Kiefer W 1983 *Chem. Phys. Lett.* **94** 41

[9] Cabaco M I, Besnard M and Yarwood J 1992 *Mol. Phys.* **50** 139

[10] Singh R K, Bhriguvansh P, Asthana B P and Verma A L 1998 *Chem. Phys. Lett.* **296** 611

[11] Schlücker S, Singh R K, Asthana B P, Popp J and Kiefer W 2001 *J. Phys. Chem.* A **105** 9983

[12] Schlücker S, Koster J, Singh R K and Asthana B P 2007 *J. Phys. Chem.* A **111** 5185

[13] Schlund S, Mladenovic M, Basílio Janke E M, Engels B and Weisz K 2005 *J. Am. Chem. Soc.* **127** 16151

[14] Andrei H S, Solcà N and Dopfer O 2006 *Chem. Phys. Chem.* **7** 107

[15] Pimentel G C and McClellan A L 1960 *The Hydrogen Bond* (San Frecisco: Freeman)

[16] Asthana B P and Kiefer W 1992 *Vibrational Spectra and Structure* (Amsterdam: Elsevier) p. 67

[17] Yang Y, Liu Y L, Zhu K, Zhang L Y, Ma S Y, Liu J and Jiang Y J 2010 *Chin. Phys.* B **19** 037802

[18] Zhang S A, Zhang H, Wang Z G and Sun Z R 2010 *Chin. Phys.* B **19** 043201

[19] Ouyang S L, Wu N N, Sun C L, Liu J Y and Gao S Q 2010 *Chin. Phys.* B **19** 093103

[20] Martin D and Hauthal H G 1975 *Dimethyl Sulfoxide* (Berlin: Van Nostrand Reinhold) p. 49

[21] Sastry M I S and Singh S 1984 *J. Raman Spectrosc.* **15** 80

[22] Wulf A and Ludwig R 2006 *Chem. Phys. Chem.* **7** 266

[23] Stafford G J, Schaffer P C, Leung P S, Doebbler G F, Brady GW and Lyden E F X 1969 *J. Chem. Phys.* **50** 2140

[24] Bertoluzza A, Bonora S, Battaglia M A and Monti P 1979 *J. Raman Spectrosc.* **8** 231

[25] Brink G and Falk M 1970 *J. Mol. Struct.* **5** 27

[26] Soper A K and Luzar A 1992 *J. Chem. Phys.* **97** 1320

[27] Soper A K and Luzar A 1996 *J. Phys. Chem.* **100** 1357

[28] Soper A K, Luzar A and Chandler D 1993 *J. Chem. Phys.* **99** 6836

[29] Cabral J T, Luzar A, Teieira J and Bellissent-Funel M C 2000 *J. Chem. Phys.* **113** 8736

[30] Ouyang S L, Zhou M, Cao B, Lu G H, Gao S Q and Li Z W 2008 *Chem. J. Chin. Univer.* **29** 2055

[31] Frisch M J, Truck G W, Schlegel H B, Scuseria G E, Robb M A, Cheeseman J R, Zakrzewski V G, Montgomery J A Jr, Stratmann R E, Burant J C, Dapprich S, Millam J M, Daniels A D, Kudin K N, Strain M C, Farkas O, Tomasi J, Barone V, Cossi M, Cammi R, Mennucci B, Pomelli C, Adamo C, Clifford S, Ochterski J, Petersson G A, Ayala P Y, Cui Q, Morokuma K, Malick D K, Rabuck A D, Raghavachari K, Foresman J B, Cioslowski J, Ortiz J V, Boboul A G, Stefnov B B, Liu G, Liaschenko A, Piskorz P, Komaromi L, Gomperts R, Martin R L, Fox D J, Keith T, AlLaham M A, Peng C Y, Nanayakkara A, Gonzalez C, Challacombe M, Gill P M W, Johnson B, Chen W, Wong M W, Andres J L, Gonzalez C, Head-Gordon M, Replogle E S and Pople J A *GAUSSIAN 03*, revision A.1 ed. Guassian, Inc., Pittsburgh, PA, 2003

[32] Wakabayashi K, Maeda Y, Ozutsumi K and Ohtaki H 2004 *J. Mol. Liq.* **110** 43

[33] Oxtoby D W 1979 *Adv. Chem. Phys.* **40** 1

[34] Ojha A K, Srivastava S K, Singh R K and Asthana B P 2006 *J. Phys. Chem.* A **110** 9849

[35] Bondarev A F and Mardaeva A I 1973 *Opt. Spectrosc.* **35** 67